GEOPHYSICAL RESEARCH LETTERS, VOL. 28, NO. 8, PAGES 1619-1622, APRIL 15, 2001

Synoptic sections of the Denmark Strait Overflow

James B. Girton and Thomas B. Sanford

Applied Physics Laboratory and School of Oceanography, University of Washington

Rolf H. Käse

Institut für Meereskunde an der Universität Kiel

Abstract. We report on a rapid high-resolution survey of the Denmark Strait overflow (DSO) as it crosses the sill, the first such program to incorporate full-water-column velocity profiles in addition to conventional hydrographic measurements. Seven transects with expendable profilers over the course of one week are used to estimate volume transport as a function of density. Our observations reveal the presence of a strongly barotropic flow associated with the nearly-vertical front dividing the Arctic and Atlantic waters. The seven-section mean transport of water denser than $\sigma_\theta = 27.8$ is 2.7 ± 0.6 Sv, while the mean transport of water colder than 2.0°C is 3.8 ± 0.8 Sv. Although this is larger than the 2.9 Sv of $\theta < 2$°C water measured by a 1973 current meter array, we find that a sampling of our sections equivalent to the extent of that array also measures 2.9 Sv of cold water. Both the structure and magnitude of the measured flow are reproduced well by a high-resolution numerical model of buoyancy-driven exchange with realistic topography.

Introduction

The southward flow of dense water through the Denmark Strait, between Greenland and Iceland, is one of the most localized and energetic legs of the global thermohaline circulation, producing a major ingredient of the North Atlantic Deep Water observed throughout the world's oceans. The ICES "OVERFLOW '73" experiment (hereafter O73) showed that the DSO is fast (frequently over 1 m s^{-1}), highly variable on timescales of 2–5 days and steady over longer periods [*Ross*, 1984]. Tides play only a small role, accounting for 2–10% of the variance in the O73 velocities. The longer-duration MONA array about 100 km downstream corroborated these conclusions and revealed a lack of variability on seasonal timescales [*Aagaard and Malmberg*, 1978]. Further downstream, current meters deployed intermittently from 1986 to the present on the Greenland slope off Angmagssalik have observed no significant interannual transport variability [*Dickson and Brown*, 1994].

Measurements

In attempt to better characterize the structure and evolution of the DSO, we conducted an extensive survey from the R/V *Poseidon* in September of 1998, using primarily expendable instruments to maximize synopticity. We report here on the seven sections nearest the sill (Figure 1), with three of these crossing the saddle point (t1u, t2u, t3u), two at approximately the O73 array location (xo1, xo4) and two oriented diagonally in the intervening region (xo2, xo3).

The velocity sections, shown in Plate 1, are a combination of data from the shipboard acoustic Doppler current profiler (ADCP) with high resolution in the upper 300–400 m of the water column and full-depth expendable current profilers (XCP) at locations marked by dotted lines. Absolute ADCP velocities were obtained using differential GPS navigation and used to reference the XCP profiles of relative velocity where they overlap. Combined ADCP, GPS and XCP random errors yield a standard error in the estimated water velocity that varies with GPS quality and ship motion but is about 0.02 m s^{-1} for most of the sections discussed here. Comparison of a few nearly-simultaneous conductivity-temperature-depth (CTD) profiles from both expendable (XCTD) and cable-lowered instruments indicate that salinity and temperature from the XCTD are accurate to within 0.02°C and 0.02 PSU (corresponding to a density accuracy of 0.02 kg m^{-3}) after correction for temperature *vs.* conductivity sensor time lags and systematic temperature and conductivity biases within the batch used for this study.

Results

All seven sections show the dense water banked against the Greenland side of the strait, as expected for an outflow in which the Coriolis acceleration is important. Another notable feature of all sections is the nearly barotropic (depth-independent) nature of the velocity, extending high above the dense layer, and the thin width (~15–20 km) of the maximum outflow. This jet appears to be a persistent feature of the DSO, having been previously observed in near-surface currents [*Fristedt et al.*, 1999].

Transport

DSO transport is often defined as all water denser or colder than a specified value. Transports obtained in this way from a range of densities are shown in Plate 1 (panel i). The most commonly-used criteria have been $\sigma_\theta > 27.8$ (where $\sigma_\theta + 1000$ equals potential density in kg m^{-3}) [*Dickson and Brown*, 1994] and $\theta < 2$°C [*Ross*, 1984]. Table 1 reports the transports through each section in Plate 1, computed using these two criteria. (Alternatively, using $\theta < 3$°C [*Saunders*, 2000], our mean and median transports become 4.0 Sv and 4.3 Sv, respectively.) The largest contributors to the error estimates shown in Table 1 are uncertainties in interpolation in near-bottom regions between profiles of differing depth and extrapolation beyond the ends of sec-

Paper number 2000GL011970.
0094-8276/01/2000GL011970$05.00

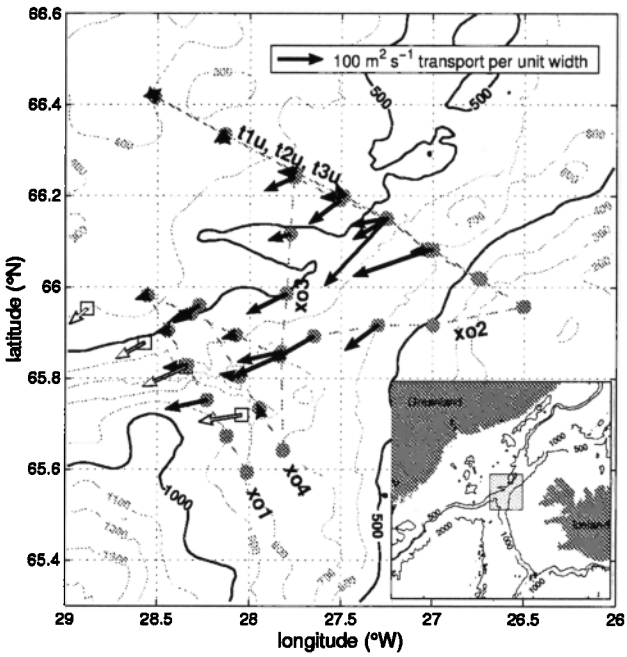

Figure 1. Locations of 1998 XCP/XCTD drops (dots) and 1973 current meters (squares). Open arrows show 5-week means of cold ($\theta < 2°C$) water transport from the current meters. Solid arrows show dense ($\sigma_\theta > 27.8$) water transport from single profiles. Dots without arrows indicate that no overflow water was detected. Note that section xo2 has a bend in the middle and extends as far as the northern end of xo1. Bathymetry in meters from the *Smith and Sandwell* [1997] database is shown.

tions. In only a few cases do the contributions from random instrumental (XCP, ADCP, GPS) errors make a noticeable difference in the error estimates. Uncertainty in the mean transport is clearly due more to natural variability than to either interpolation or measurement errors. We estimate this uncertainty on the last row of Table 1 by assuming a steady variability equal to the standard deviation of our measurements and an estimated 5 degrees of freedom, resulting from the close temporal spacing of some of our 7 sections relative to the integral timescale of 10 hours present in the O73 data.

Interestingly, the highly barotropic nature of the flow at the sill implies that over 80% of the overflow transport in our sections can be accounted for using only near-surface velocities and the depth of the DSOW interface. Since a number of hydrographic surveys have been made in the sill region from ships equipped with ADCP instruments, a larger database of transport estimates could be constructed in this manner. However, this would not work further downstream along the Greenland slope, once the overflow has begun its rapid descent. In addition to the greater water depth and smaller fraction covered by the ADCP, the flow becomes more bottom-intensified in this region, making the barotropic component relatively less important.

We have examined the original O73 current meter records (C. K. Ross, personal communication, 1998) and found hourly transports ranging from 0.2–8.5 Sv. The distribution is skewed heavily towards the lower values, with a large number of points falling within a low-transport mode around 1.5 Sv, as well as a substantial number distributed throughout higher values, corresponding to high-transport episodes at intervals of 2–5 days. The mean and median of the unfiltered hourly transports are 2.8 and 2.2 Sv, respectively. The cumulative probability distribution of these transports is shown in Figure 2.

Subsampling

In order to compare our measurements and O73, we performed two subsampling exercises. The first was to use observations at the same spacings and heights off the bottom as the O73 array instruments to estimate an "array-sampled" version of $\theta < 2°C$ transport in each of our velocity and temperature sections. The resulting transports are shown in the rightmost column of Table 1. The points sampled on those sections not lying close to the O73 array were chosen by projection along topography as realistically as possible. The cumulative probability distribution from these array-sampled values (Figure 2) lies almost on top of that from the O73 array, with a Kolmogorov-Smirnov (K-S) test [*Press et al.*, 1995] finding less than 1% significance to the difference between the two. The mean of the array-sampled values in Table 1 also falls very close to the mean of the $\sigma_\theta > 27.8$ values, supporting the case for comparing the O73 result with density-defined overflow transport measurements further downstream [*Dickson and Brown*, 1994].

The second exercise repeatedly picked 7 values at random from the O73 transport timeseries to construct probability distributions for the 7-sample maximum, minimum, mean, median and standard deviation. We found that each of these statistics from our array-sampled values fell within a $\pm 1\sigma$ (67%) probability range from the O73 distribution. This, along with the K-S test mentioned above, shows that no significant difference has been found between the magnitude and variability of transport in our measurements and that observed during the O73 period, 25 years earlier.

Table 1. DSO Transport

	$\sigma_\theta > 27.8$	$\theta < 2°C$	array-sampled
t1u	2.3 ± 0.2	4.4 ± 0.2	1.5
xo1	1.3 ± 0.2	1.4 ± 0.2	2.0
xo2	1.6 ± 0.2	1.9 ± 0.2	1.0
t2u	2.7 ± 0.1	3.1 ± 0.1	2.6
t3u	4.8 ± 0.3	5.8 ± 0.3	6.2
xo3	4.2 ± 0.2	5.4 ± 0.3	4.1
xo4	1.9 ± 0.1	4.6 ± 0.3	3.0
mean	2.7	3.8	2.9
median	2.3	4.4	2.6
$\frac{\text{st. dev.}}{\sqrt{5}}$	± 0.6	± 0.8	± 0.8

All values are in Sverdrups ($1\,\text{Sv} = 10^6\,\text{m}^3\,\text{s}^{-1}$). Error estimates include the effects of interpolation/extrapolation choices, instrumental errors and ADCP mounting angle uncertainty, representing the authors' best attempts to gauge the $\pm 1\sigma$ (67% confidence) level of each synoptic transport measurement. Array-sampled values were estimated by subsampling the sections at the equivalent depths and distances of the O73 array and computing $\theta < 2°C$ transport.

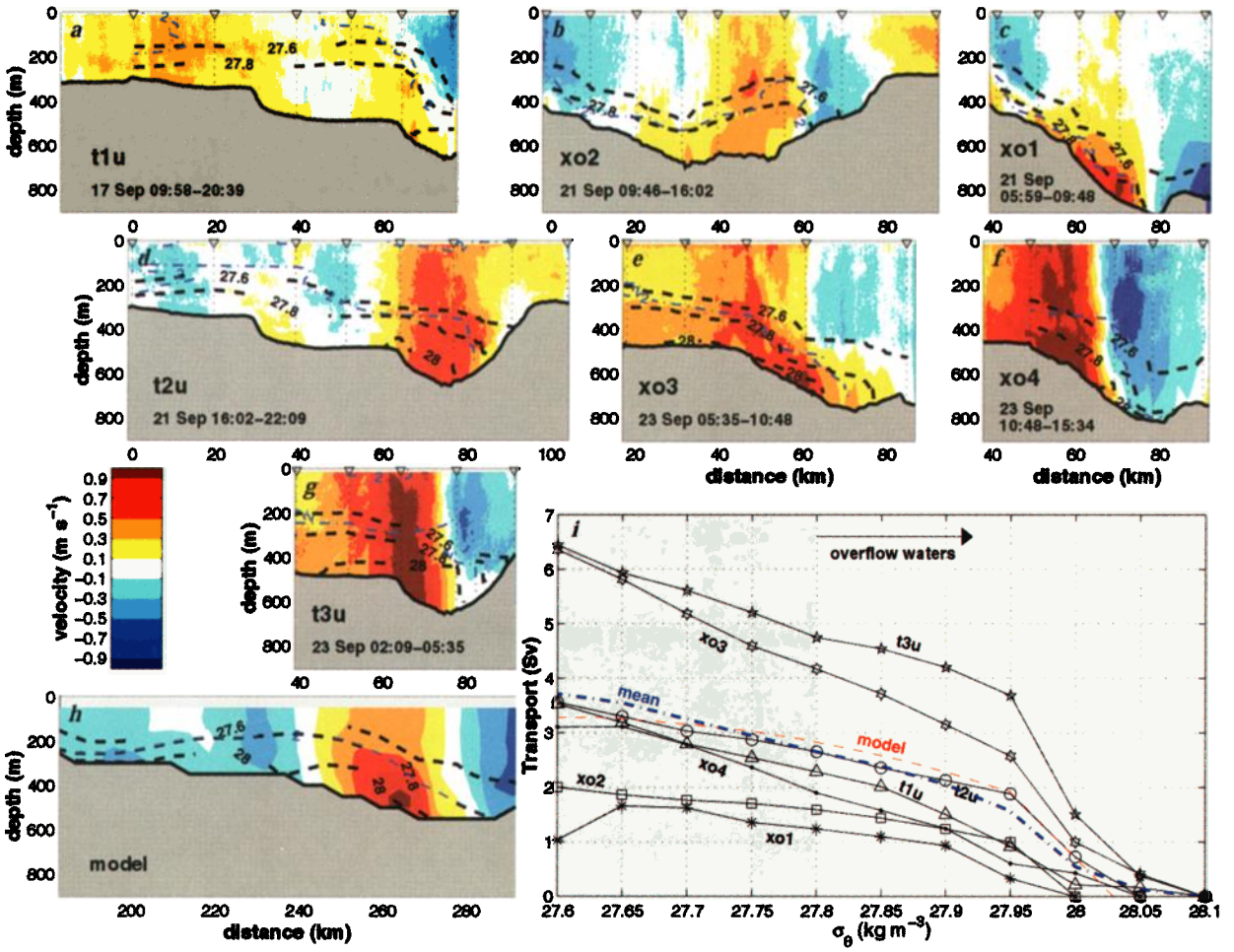

Plate 1. (*a–g*) Seven snapshots from the sections in Figure 1. Similar sections are aligned vertically for comparison. Greenland lies to the left and Iceland to the right. The XCP/ADCP velocity component normal to a best-fit line along the section is shaded in color. Positive velocities are directed toward the viewer, *i.e.*, southwestward. Three isopycnals (σ_θ = 27.6, 27.8 and 28.0, dashed) and one isotherm (2°C, dot-dashed) from XCTD profiles are also shown. (*h*) Single snapshot from the equivalent location in the *Käse and Oschlies* [2000] (KO) model. (*i*) Cumulative through-section transport of dense water in each section, including the 7-section mean (dot-dashed) and a 22-day average from the model (dashed). Enlarged figures and additional information can be obtained from *http://www.apl.washington.edu/dso.*

Model Comparison

A regional sigma-coordinate model with realistic topography and parameters appropriate to the DSO [*Käse and Oschlies*, 2000, hereafter KO] replicates many of the features present in our observations. The model is initialized in a "dambreak" scenario, with dense water (σ_θ = 28.03) filling the northern basin to 50 m below the surface and light water (σ_θ = 27.45) elsewhere. A barrier at the sill is removed and the dense water spills into the southern basin, establishing a steady overflow with sloping density interface, dominantly barotropic velocity structure with some bottom intensification and recirculations on both sides of the outflowing jet (Plate 1, panel h). A 22-day mean of the model's transport of dense water across the sill, shown by the dashed line in Plate 1 (panel i), lies very close to the mean transport from our seven sections. This agreement, despite the model's closed-basin geometry, lack of surface forcing and simplified initial density structure, indicates the degree to which the overflow represents a purely source-driven flow controlled by topography.

The geostrophic transport of a dense layer through a constriction wider than the baroclinic Rossby radius is limited by hydraulic and potential vorticity constraints to a value of $\frac{g' h_u^2}{2f}$, where h_u is the height above the sill of the upstream layer interface [*Whitehead*, 1998]. Using the conditions in the northern basin during our measurement program ($g' = 4.3 \times 10^{-3}$ m s^{-2} and h_u = 550 m) gives a maximal transport of 4.9 Sv. Depending on the choice of hydrographic stations used, this estimate could be as high as 5.3 Sv, but is certainly at least 50% higher than both the observed and modeled transports.

The discrepancy is probably due to frictional or time-dependent effects, both of which are substantially present in the model and in the observed overflow. KO show that the model transport reaches the maximal value at times but is often restrained by a geostrophic front created by flow recirculation towards Greenland at the sill. In addition, estimates of shear stress from logarithmic fits to the bottom 20 m of XCP velocity profiles suggest that friction plays an important role in the dynamics of the overflow. Bottom

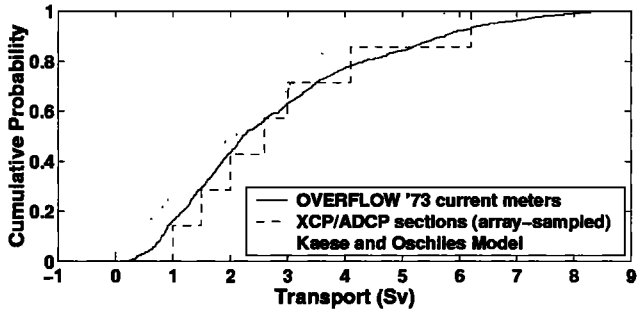

Figure 2. Cumulative probability distributions for time-varying θ<2°C transport estimates showing comparison among O73 array, 7 synoptic sections and KO model.

stresses in the sections discussed here range from 0.1–7.7 Pa (median of 0.4 Pa), and a fit *vs.* the squared velocity at a height of 50 m above the bottom (high enough to be above the boundary layer but still within the overflow water) yields an estimated drag coefficient of 3.1×10^{-3}. These values are comparable to those observed in the Mediterranean outflow [*Johnson et al.*, 1994], in which it has been shown that both bottom and interfacial stresses are important elements of the momentum balance in the descending plume. Interestingly, significant differences in the KO model overflow transport are not found between runs conducted using different values of the (linear) bottom friction parameter. This may be because the "high" friction used (corresponding to 0.2 Pa at 0.5 $m\,s^{-1}$) is still too low. The expected influence of bottom friction on transport is not clear, however, and it may still be possible to achieve maximal flow in spite of substantial friction if geostrophic constraints are more important than inertial ones.

Conclusions

Our estimate of the mean transport of 2.7±0.6 Sv of dense water through the Denmark Strait, made over a 1-week period, is essentially identical to the 2.9 Sv of cold water measured in 1973 [*Ross*, 1984]. In fact, while our measurements show that the $\theta < 2°C$ criterion encompasses a substantial amount of non-overflow water, the positioning of the O73 array was able to give a reasonable measurement of overflow transport. Although both the O73 program and our new measurements took place in late summer and neither was of particularly long duration, the equivalent results do add more evidence to support the view of the DSO as an unchanging, hydraulically-controlled flow on timescales longer than a few days. This view is supported by current meter studies in the DSO to date, both upstream and downstream of the sill, which have been unable to identify significant seasonal or interannual variability [*Aagaard and Malmberg*, 1978; *Dickson and Brown*, 1994].

Recent hydrographic studies of the dense water downstream have brought the steady-state into question [*Bacon*, 1998] but are vulnerable to errors due to assumptions about geostrophic reference levels. In addition, multi-year changes in atmospheric forcing and convective activity of the Nordic Seas [*Dickson et al.*, 1996] are likely to have some effect on the DSO, and it is surprising that this has not yet been seen. Perhaps the answer lies in the substantial variety of source waters available to supply the overflow (generated by processes in the Arctic Ocean, Greenland Sea, Iceland Sea and East Greenland Current [*Rudels et al.*, 1999]) combined with the restraint imposed on the flow by the shoaling and constriction in the Strait.

Acknowledgments. The authors would like to thank John Dunlap and Janko Hauser for providing invaluable assistance with the experiment and data analysis. This work was supported by the National Science Foundation and the German SFB-460 program.

References

Aagaard, K., and S.-A. Malmberg, Low-frequency characteristics of the Denmark Strait Overflow, *ICES CM 1978/C:47*, Int. Counc. for the Explor. of the Sea, Copenhagen, 1978.

Bacon, S., Decadal variability in the outflow from the Nordic seas to the deep Atlantic Ocean, *Nature*, *394*, 871–874, 1998.

Dickson, R., J. Lazier, J. Meincke, P. Rhines, and J. Swift, Long-term coordinated changes in the convective activity of the North Atlantic, *Progr. Oceanogr.*, *38*, 241–295, 1996.

Dickson, R. R., and J. Brown, The production of North Atlantic Deep Water: Sources, rates, and pathways, *J. Geophys. Res.*, *99C*, 12319–12341, 1994.

Fristedt, T., R. Hietala, and P. Lundberg, Stability properties of a barotropic surface-water jet observed in the Denmark Strait, *Tellus*, *51A*, 979–989, 1999.

Johnson, G. C., T. B. Sanford, and M. O'Neil-Baringer, Stress on the Mediterranean outflow plume I: Velocity and water property measurements, *J. Phys. Oceanogr.*, *24*, 2072–2083, 1994.

Käse, R. H., and A. Oschlies, Flow through Denmark Strait, *J. Geophys. Res.*, *105C*, 28527–28546, 2000.

Press, W. H., S. A. Teukolsky, W. T. Vetterling, and B. P. Flannery, *Numerical Recipes in C: The Art of Scientific Computing*, 2nd ed., Cambridge University Press, 1995.

Ross, C. K., Temperature–salinity characteristics of the "overflow" water in Denmark Strait during "OVERFLOW '73", *Rapp. P.-v. Réun. Cons. int. Explor. Mer.*, *185*, 111–119, 1984.

Rudels, B., H. J. Friedrich and D. Quadfasel, The Arctic circumpolar boundary current, *Deep-Sea Res. II*, *46*, 1023–62, 1999.

Saunders, P., The dense northern overflows, in *Ocean Circulation and Climate*, edited by G. Siedler, J. Church, and J. Gould, Academic, in press, 2000.

Smith, W. H. F., and D. T. Sandwell, Global sea floor topography from satellite altimetry and ship depth soundings, *Science*, *277*, 1956–1962, 1997.

Whitehead, J. A., Topographic control of oceanic flows in deep passages and straits, *Rev. Geophys.*, *36*, 423–440, 1998.

J. B. Girton and T. B. Sanford, Applied Physics Laboratory and School of Oceanography, University of Washington, Seattle, WA 98105-6698. (e-mail: girton@apl.washington.edu)

R. H. Käse, Institut für Meereskunde an der Universität Kiel, 24105 Kiel, Germany.

(Received May 29, 2000; accepted January 02, 2001)